Local Photocarrier Dynamics in CdTe Solar Cells Under Optical and Electron Beam Excitations

Heayoung P. Yoon[1,2], Paul M. Haney[1], Yohan Yoon[1,2], Sangmin An[1,2], James I. Basham[1], and Nikolai B. Zhitenev[1]

[1]National Institute of Standards and Technology, Gaithersburg, MD, 20889, USA, [2]Maryland NanoCenter, University of Maryland, College Park, MD 20742, USA

***Abstract* — We investigate local carrier dynamics in *n*-CdS / *p*-CdTe solar cells, where the electron-hole pairs are generated by either near-field optical illumination or highly focused electron beam excitation. A focused ion milling process was used to prepare a smooth surface and cross-sections of the devices. The spatially resolved photocurrent images confirm high carrier collection efficiencies at grain boundaries. An analytical model was used to extract material parameters at the level of single grains. We find that the minority carrier diffusion length and device parameters extracted from the local measurement techniques are in excellent agreement, but can be different determined from macro-scale measurements.**

I. Introduction

Polycrystalline thin film photovoltaic (PV) technologies have shown great promise for solar energy harvesting using inexpensive PV materials, currently reaching a power conversion efficiency of 21.0 % for cadmium telluride (CdTe) and 21.7 % for copper indium gallium selenide (CIGS) solar cells [1]. To achieve the maximum efficiency of ≈ 30 % possible for these technologies, considerable efforts have been made to understand the physical mechanisms that limit cell performance. Large-area optical characterizations are well-established techniques that diagnose optical and electrical losses of PV devices. Among them, external quantum efficiency (EQE) measures the ratio of the collected charged carriers to the incident photons on a solar cell at different wavelengths, showing how effectively a photovoltaic device converts sunlight into electricity throughout the spectrum. Light absorption varies as a function of the wavelength of incident light (e.g., larger absorption volume at longer wavelengths) and thus the EQE data provides rich information about each layer and interface of the solar cell [2].

While extremely informative, the macro-scale (> 1 mm) optical data alone are not sufficient to understand the impact of microstructures (< 1 μm) on their operation and performance in CdTe or CIGS [3]. Local quantum efficiency can be measured by near-field scanning optical microscopy (NSOM). In this technique, local electron-hole pairs are generated by light injected through a small aperture (< 200 nm in diameter). Spatially resolved local quantum efficiency can be obtained by varying the wavelength of light. Alternatively, electron-beam induced current (EBIC) is a complementary technique that provides higher spatial resolution (<20 nm). In addition, this technique allows systematic controls of the carrier generation (three orders of magnitude) and of the size of interaction volume (tens of nm to a few μm), well-suited for quantitative study. As in NSOM, the generated electron-hole pairs are rapidly separated at Schottky barrier or *p*-*n* junction before they recombine, and the carriers collected by the contacts produce a current. Although EBIC does not represent a direct map of the quantum efficiency, the correlation between EBIC grain boundary contrast and device performance strongly suggests that this technique reveals meaningful and important material characteristics [4, 5]

In this work, we perform cross-sectional photocurrent measurements using optical and electron beam excitations. By fitting the line-scans using analytical models, materials parameters are extracted and compared to the corresponding macro-scale optical data. We discuss possible origin of the discrepancy between macro- and micro-scale properties.

II. Experimental

Standard semiconductor processes were used to fabricate Ohmic metal contacts on the surface of *p*-CdTe / *n*-CdS junctions extracted from a commercial solar panel [4]. Cross-sections of the devices were obtained by a focused ion beam milling (FIB) technique. In this process, a beam of Ga ions ($V_{b,\,Ga}$ = 30 keV; $I_{b,Ga}$ = 2.5 nA) is precisely controlled to etch away the target material, creating a smooth surface. The acceleration voltage and the beam current of the electron beam and the ion beam used in this work are nominal values. The measured fluctuation of the beam current is < 5%. Topography and NSOM measurement were performed using a tapping mode atomic force microscopy (AFM) system. Multiple single mode lasers (405 nm, 520 nm, 635 nm, 780 nm) were used. Acquisition of EBIC images at beam energies ranging from 1 keV to 20 keV was performed in a scanning electron microscopy (SEM) system. While the contact of TCO/*n*-CdS/indium was grounded, a Tungsten probe tip controlled by a nano-manipulator was used as a current collector from patterned metal contact to *p*-CdTe. A custom designed sample stage was used to ensure high signal-to-noise ratio within the full range of signals for low- and high keV EBIC.

III. Results and Discussion

The baseline PV performance of the extracted CdTe device was evaluated. The measured power conversion efficiency was ≈12 % with a short-circuit current (J_{sc}) of (23 ± 0.5) mA/cm^2, an open-circuit voltage (V_{oc}) of (820 ± 10) mV, and fill factor (FF) of (64 ± 3) %, indicating that the device properties are mainly preserved after the extraction processes. Standard external quantum efficiency (EQE) profiles were collected under 1 sun illumination, shown in Figure 1 (a). In this optical measurement, a ratio of the number of collected carriers to the number of absorbed photons is recorded at each wavelength. A complete QE analysis is used to identify the optical and electronic losses reducing J_{sc} and to extract the materials parameters. By fitting the variation of the QE from 650 nm to 800 nm, we estimated the minority carrier diffusion length (L_n) to be approximate 1µm. Taking the average grain size of ≈1 µm (Figure 1 b), the typical beam (≈2 mm in diameter) interacts with over ≈10^6 grains.

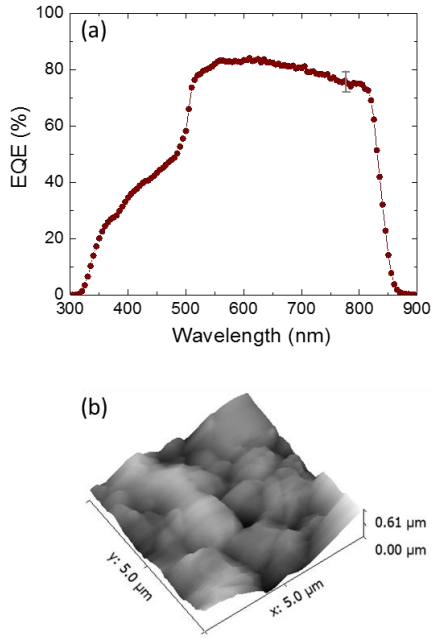

Fig. 1. (a) External quantum efficiency profile of a *n*-CdS / *p*-CdTe extracted from a commercial solar panel. The estimated minority carrier diffusion length (650 nm to 800 nm) is ≈ 1 µm. (b) An AFM image displays the peak-to-valley surface roughness of the CdTe ≈ 0.6 µm. The typical grain size of the CdTe is ≈1 µm.

In order to correlate the macro-scale PV properties to microstructural properties, we perform near-field scanning optical microscopy. In contrast to the EQE, the electron-hole pairs are locally generated by the light injected through a small aperture (< 200 nm in diameter). Cross-sectional devices were used to map the local responses throughout the entire *p-n* junction region. The topography of the FIB milled section is very smooth (peak-to-valley roughness < 20 nm). Figure 2 (a) and (b) shows the photocurrent map at 405 nm and 635 nm illumination, respectively. The spatial resolution decreases at the higher wavelength, as expected, due to the increase in the absorption depth. Nonetheless, the bright contrast at the grain boundaries indicates high carrier collection efficiency, as proposed in previous works [4, 5]. We fit the line-scan collected in a single grain bulk under the 635 nm illumination (Figure 2 c) and estimated L_n ≈ 0.6 µm ± 0.06 µm.

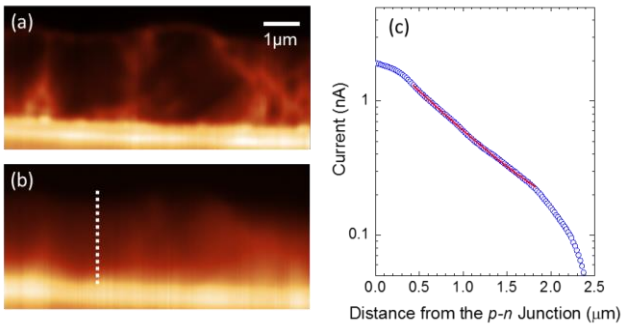

Fig. 2. Near-field scanning microscopy of a FIB prepared CdTe device. Photocurrent maps at 405 nm (a) and 635 nm (b). The estimated photon absorption depth is 100 nm and 400 nm, respectively. (c) A line-scan profile at 635 nm illumination (white dot line in b). The red line represents the model fit to extract the minority carrier diffusion length.

The spectrally resolved photocurrent images are compared to the carrier collection maps obtained by EBIC. A series of cross-sectional EBIC images were obtained by varying the acceleration voltage of the electron beam (Figure 3). The strong bright contrast at the grain boundaries reflects high carrier collection efficiencies also seen in NSOM data (Figure 2 c). Qualitatively, the 5 keV and 10 keV EBIC images are similar to that of 405 nm and 635 nm NSOM maps, respectively. This correspondence indicates that the calculated photon absorption and electron penetration depths are in good agreement.

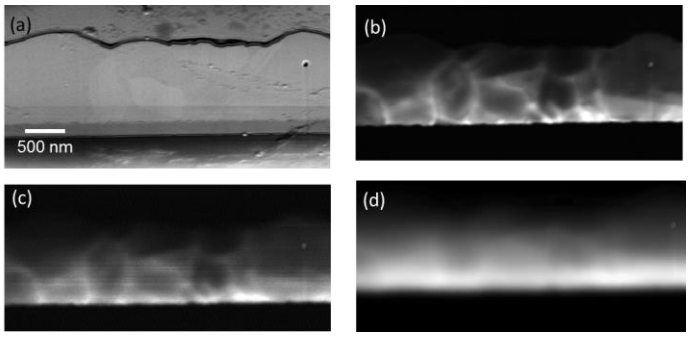

Fig. 3. (a) Cross-sectional SEM image on a FIB prepared device. Corresponding EBIC images at (b) 3 keV, (c) 5 keV, and (d) 10 keV. The calculated penetration depth in CdTe is 40 nm, 90 nm, and 310 nm at 3 keV, 5 keV, and 10 keV, respectively [7].

Both EBIC and NSOM techniques are surface sensitive owing to the carrier generation close to the exposed surface. To extract material parameters, an analytical modeling is required to de-convolute non-linear responses at different beam energies (or different wavelength) and complex signals arising from grain bulk and grain boundaries. Figure 4 (a) plots a series of EBIC line scans obtained on a large, single grain at different acceleration voltages. We estimate an uncertainty in the *p-n* junction position of 50 nm based on the discretization of the electron beam position in the line scan. For quantitative comparison, we performed least-squares fitting of the individual EBIC line scans using an analytical model [6]. Figure 4 (b) plots extracted effective minority carrier diffusion lengths at different acceleration voltages, which is quite similar to that estimated from NSOM data (Figure 2 c). However, this local value ($L_n \approx 0.6$ µm) is smaller than the value of L_n extracted from the macro-scale quantum efficiency profile ($L_n \approx 1$ µm), which would be attributed to influence of grain boundaries.

In conventional EBIC models, the carrier collection efficiency at *p-n* junction is 100 % inside the depletion region where built-in potential is present [6]. On the contrary, we found that the EBIC efficiencies extracted in our devices are well below 100 %. The measured EBIC efficiency rapidly increases with the beam voltage, indicating that a strong recombination occurs near the surface. However, the EBIC efficiency remains below 60 % even when the electron beam is injected far away from the surface. Such low EBIC efficiencies implies that some factors (e.g., recombination, screening of built-in field by generated carriers) not accounted in standard model play an important role. The source of the reduced EBIC efficiency in the depletion region is the subject of on-going work. Nevertheless, our model has shown that the diffusion length extracted in the neutral region is insensitive to enhanced recombination in the depletion region.

IV. CONCLUSIONS

In summary, we present local photocurrent measurements of a cross-sectional CdTe solar cell that were obtained by near-field optical illumination and by focused electron beam irradiation. The spatially and spectrally resolved efficiency maps confirm a higher carrier collection at grain boundaries. We estimate the minority carrier diffusion lengths of individual grains away from grain boundaries obtained from NSOM and EBIC data, showing an excellent agreement between the techniques. Local values ($L_n \approx 0.6$ µm) are smaller than the one ($L_n \approx 1$ µm) extracted from the macro-scale quantum efficiency measurement which is attributed to the contribution of grain boundaries. We find that the maximum EBIC efficiency at the *p-n* junction in the FIB prepared CdTe solar cell is significantly less than 100%, implying that the standard EBIC model is insufficient for quantitative data processing. Development of analytical models which account for surface recombination in depletion regions and screening of built-in fields from carrier accumulation are in progress.

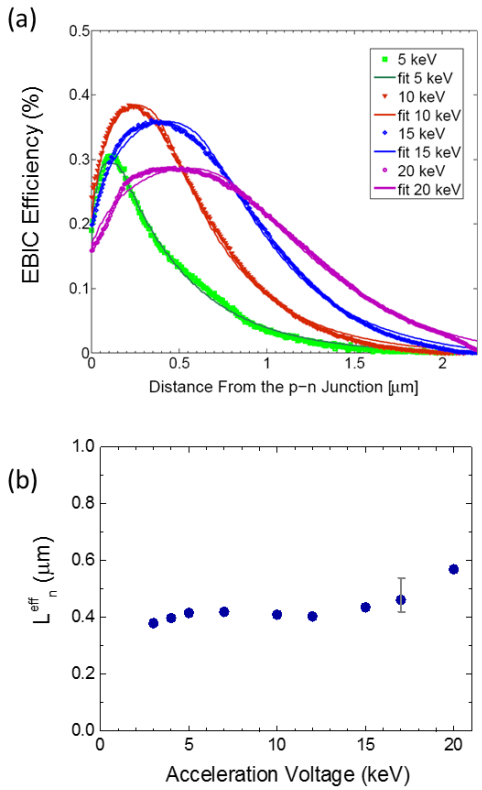

Fig. 4. (a) Solid are experimental EBIC line scans obtained for a large, single grain. (b) Estimated minority carrier diffusion lengths at different acceleration voltages.

REFERENCES

[1] Research Cell Efficiency Records (http://www.nrel.gov/ncpv/).

[2] S. S. Hegedus and W. N. Shafarman, "Thin-Film Solar Cells: Device Measurements and Analysis", Prog. Photovolt: Res. Appl., vol. 12, pp. 155–176, 2004.

[3] S. Kumar and K. Rao, "Physics and chemistry of CdTe/CdS thin film heterojunction photovoltaic devices: fundamental and critical aspects", Energy Environ. Sci., vol. 7, p.45, 2014

[4] H. Yoon *et al.*, "Local electrical characterization of cadmium telluride solar cells using low-energy electron beam", Sol. Eng. Mat. Sol. Cells, vol. 117, pp. 499-504, 2013.

[5] J. D. Poplawsky *et al.*, "Direct Imaging of Cl- and Cu-Induced Short-Circuit Efficiency Changes in CdTe Solar Cells", Adv. Energy Mater., 1400454, 2014.

[6] P. M. Haney, H. P. Yoon, P. Koirala, R. W. Collins, N. B. Zhitenev, "Electron beam induced current in the high injection regime", arXiv:1410.4435v1, 2014.

[7] D. Drouin et al., "CASINO V2.42 - A Fast and Easy-touse Modeling Tool for Scanning Electron Microscopy and Microanalysis Users", Scanning 29, 2007, pp. 92-101.